

# Magnetic enhancement of Chinese loess—the role of $\gamma\text{Fe}_2\text{O}_3$ ?

John K. Eyre and John Shaw

Geomagnetism Laboratory, Oliver Lodge Laboratories, PO Box 147, Oxford Street, Liverpool L69 3BX, UK

Accepted 1993 October 14. Received 1993 October 14; in original form 1993 April 30

## SUMMARY

Various mechanisms have been proposed for the observed link between palaeoclimate and magnetic susceptibility in the Chinese loess. Many authors have recently pointed to the controlling influence that ultrafine (stable single domain/superparamagnetic) magnetite/maghemite has on the magnetic susceptibility signal. However, there is still no clear evidence as to the origin of this susceptibility-enhancing magnetic fraction. We have collected samples from two sites representing the range of magnetic susceptibilities to be found in the Chinese loess record. Magnetic measurements indicate that susceptibility enhancement, throughout the loess plateau, is associated with the concentration of a ferrimagnetic fine fraction. This magnetic fraction has a uniform, non-variable grain-size distribution which spans the stable single-domain/superparamagnetic boundary. High-field thermomagnetic analysis reveals a trend in behaviour with increasing susceptibility, towards linear, more reversible curves. We propose that both the particular grain size of the enhanced ferrimagnetic fraction and thermomagnetic reversibility, can be explained by size-induced phase transitions in  $\text{Fe}_2\text{O}_3$ , which results in maghemite being the energetically favoured phase for certain grain sizes. Thus, the production of  $\text{Fe}_2\text{O}_3$ , which spans this grain-size range, is the only requirement for magnetic enhancement in the loess.

**Key words:** China, loess, magnetic susceptibility, mineralogy.

## INTRODUCTION

It is generally accepted that Chinese loess/palaeosol sequences contain detailed information on the evolution of climate over the past 2.5 Ma (Liu *et al.* 1985). The most persuasive evidence for this is the presence of numerous buried soil (palaeosol) horizons reflecting climatic conditions that have fluctuated between conditions favourable (warm/wet) and less favourable (cold/dry) for soil formation. Further, a strong correlation exists between the loess magnetic susceptibility and deep-sea oxygen isotope records (a well-regarded palaeoclimatic indicator) (Heller & Liu 1986), suggesting that climate has had a significant impact on the magnetic mineralogy of the loess.

Some possible mechanisms for a climatic influence on magnetic susceptibility are summarized below.

(1) A constant influx of magnetic material from a remote source is diluted by virtually non-magnetic loess. The input of loess material is modulated by variations in wind velocity and/or frequency, which are in turn influenced by climatic variations. Thus, the concentration of magnetic material is related to climatic change (Kukla *et al.* 1988).

(2) There is a bulk grain size, and associated magnetic grain-size variation in source material, that is dependent on palaeo-wind velocities (Rolph *et al.* 1993).

(3) Wind circulation patterns may change over glacial/interglacial cycles. Source areas for loess may change as a consequence, influencing magnetic mineralogy, magnetic grain size and concentration.

(4) The possibility of *in situ* production of magnetite/maghemite by chemical, biochemical or biogenic processes has been well documented (Taylor & Schwertmann 1974a,b; Taylor, Maher & Self 1987; Maher & Taylor 1988; Anand & Gilkes 1987; Fassbinder, Stanjek & Vali 1990). Rainfall and temperature are likely to have a significant influence on such processes.

(5) In the central loess plateau the hard carbonate concretions and calcrete horizons indicate that leaching of carbonate has occurred (Guo, Nicolas & An 1991). The processes of carbonate leaching and sediment compaction have an obvious effect on the concentration of magnetic minerals (Heller & Liu 1984). Again, temperature and rainfall are likely to be the controlling factors.

If magnetic susceptibility is taken as a measure of climatic

intensity (i.e. on a scale from cold, dry and windy to warm, wet and less windy), then it is important to understand the underlying physical reasons for magnetic susceptibility enhancement. We can attempt this by observing the change in other magnetic parameters with susceptibility.

## SAMPLES

The Chinese loess plateau lies in the north-west of the country, bounded by the Tibetan plateau to the west and the Qinling mountains to the south (Fig. 1). The thickest loess deposits in the world (>300 m) can be found in the north-west of the plateau. From here, the loess thins towards the south-east and the mean grain size decreases (Liu 1985), supporting a source area in the cold deserts bounding the north and western edges of the loess plateau.

Lanzhou is situated in Gansu province, in the far west of China on the edge of the Tibetan plateau, at an altitude of 1500 m. The loess profile at Jiuzhoutai Mountain (JZT), Lanzhou, is greater than 320 m in thickness. There is some debate over the basal age of the section. Magnetostratigraphic dating by Burbank & Li (1985) and by Rolph *et al.* (1989) have produced dates of 1.4 and 2.4 Ma respectively; the discrepancy arising from their attempts to decipher the complex reversal record. The palaeosols within the loess profile are visually indistinct and have only weakly enhanced susceptibilities.

In Xian in central China, at the southern edge of the loess plateau, climatic conditions were much warmer and more

humid than in Lanzhou. The loess at Duanjiapo (DJP) is 120 m in thickness. A basal age of 2.5 Ma (Zheng, An & Shaw 1992) has been proposed based on the Matuyama/Gauss magnetic polarity reversal measured in the loess, ~1 m above the pliocene 'Red Clays'. The loess profile contains visually distinct dark reddish-brown palaeosol horizons which have strongly enhanced susceptibilities. Often palaeosols are underlain with carbonate concretion horizons or zones that can be up to 1 m in thickness.

The lowest magnetic susceptibilities (in 'loess') in the DJP section are comparable to the highest JZT susceptibilities (in 'palaeosol'). This highlights the fact that the term 'palaeosol' has little meaning, on a (loess) plateau-wide scale, when comparing material and magnetic properties. To avoid confusion, the term 'loess' is subsequently adopted to describe all material in the loess record.

A selection of samples was collected, spanning the complete age and range of materials to be found in both sections. The very different loess characteristics between the two sections is believed to reflect the superimposition of a local climate regime on larger scale, global, glacial/interglacial climatic fluctuations (Maher & Thompson 1991; Rolph *et al.* 1993). At Lanzhou, the local climatic regime resulted in the predominance of cold, dry and windy conditions throughout the history of loess deposition. On the other hand, warmer, wetter and less windy conditions prevailed at Xian.

## ROOM-TEMPERATURE MAGNETIC MEASUREMENTS

### Susceptibility

Magnetic susceptibility was measured at two frequencies (0.43 kHz and 4.3 kHz) using a Bartington dual-frequency probe. The change in susceptibility, when measured at the two frequencies (frequency-dependent susceptibility  $X_{fd}$ ), reflects the proportion of ferrimagnetic grains at the room-temperature superparamagnetic threshold. ( $X_{fd}$  (per cent) =  $100 \times (X_{lf} - X_{hf})/X_{lf}$  where  $X_{lf}$  and  $X_{hf}$  are the low and high frequency susceptibility, respectively.) Susceptibilities were measured for a set of samples (with a range of susceptibilities) from both sites.  $X_{fd}$  shows a trend with increasing low-frequency susceptibility ( $X_{lf}$ ) reflecting the increasing dominance of a magnetic fraction that spans the room-temperature stable single domain (SSD)/superparamagnetic (SP) boundary (Fig. 2).  $X_{fd}$  saturates at ~12 per cent, indicating that the enhanced magnetic fraction has a particular grain-size distribution, which has a 12 per cent frequency dependence.

### Hysteresis

Hysteresis loops were obtained using a Molyneux vibrating sample magnetometer (VSM). The hysteresis parameters—coercivity ( $H_c$ ), saturation magnetization ( $M_s$ ), saturation remanence ( $M_{rs}$ )—were plotted against low-field susceptibility (Fig. 3).  $H_c$  (which reflects the relative proportions of hard to soft magnetic components) decreases with increasing susceptibility but trends towards a coercivity of

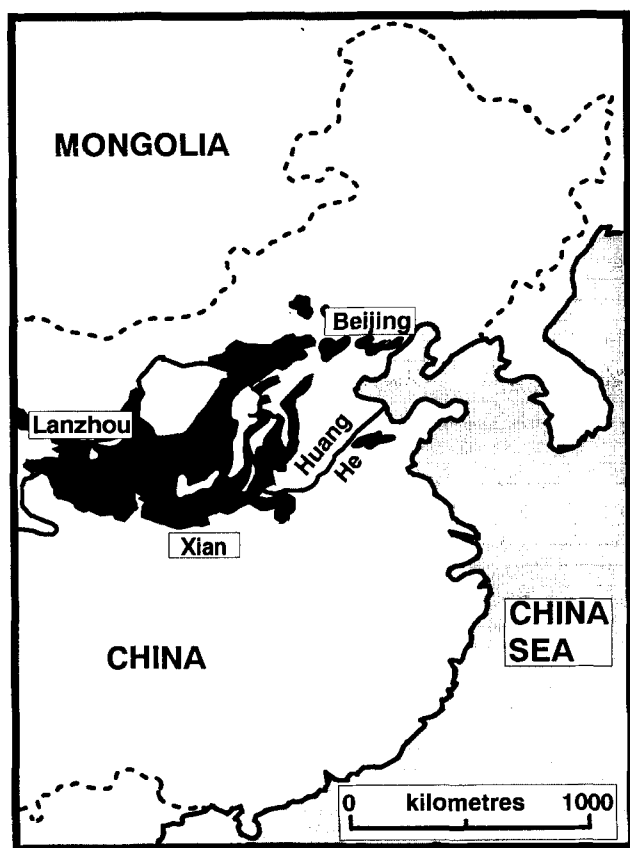
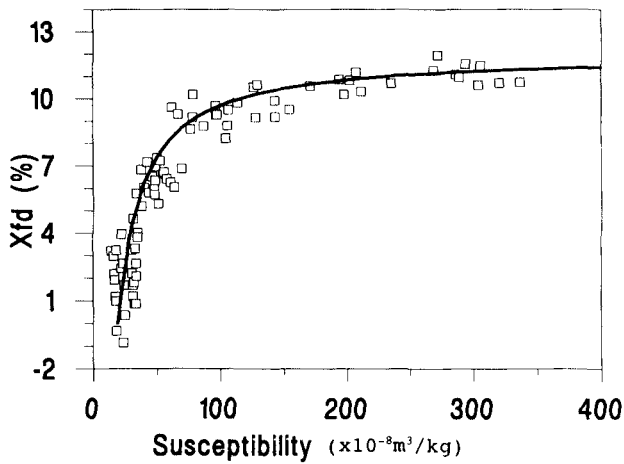


Figure 1. Location map showing the extent of loess deposits and sampling sites in northern China.



**Figure 2.** The variation in frequency-dependent susceptibility with low-frequency susceptibility. Behaviour is approximated (solid line) with the relationship  $X_{fd} = 12 - 230/X_{lf}$ .

$4.2 \times 10^3 \text{ A m}^{-1}$ . This behaviour indicates that susceptibility enhancement is associated with an enhanced magnetic fraction which has a distinct coercivity. This magnetic enhancement takes place relative to a magnetically harder 'background' component.

$M_s$  (which is a measure of the concentration of ferrimagnets) behaves linearly with susceptibility. Extrapolation reveals that the best-fit line does not pass through the origin. Saturation remanence shows similar behaviour.

The linear behaviour of  $M_s$  and  $M_{rs}$  suggests that susceptibility is controlled by ferrimagnetic concentration rather than a shift in grain size. The positive intersection of the magnetization axis indicates that the 'background' (non-enhanced) magnetic behaviour is due to material with a higher ratio of magnetization to susceptibility than the

**Table 1.** Comparison of the magnetic behaviour of the enhanced magnetic fraction (see text) with that of different ferrimagnetic size fractions. All values—ratio of saturation magnetization to low-field susceptibility ( $M_s/X_{fd}$ ), ratio of saturation remanence to low-field susceptibility ( $M_{rs}/X_{fd}$ ), and coercivity ( $H_c$ )—are in the units  $\text{A m}^{-1}$ .

	magnetite/maghemite			Enhanced fraction
	SP	SSD	MD	
$M_s/X_{fd}$	$0.15 \times 10^5$	$2.0 \times 10^5$	$1.7 \times 10^5$	$0.29 \times 10^5$
$M_{rs}/X_{fd}$	0	$2.1 \times 10^4$	$0.18 \times 10^4$	$0.44 \times 10^4$
$H_c$	0	$8 \times 10^3$	$1.6 \times 10^3$	$4.2 \times 10^3$

enhancing fraction. The ratios of  $M_s$  and  $M_{rs}$  to susceptibility (taken from the slopes) and the limiting value of coercivity (Table 1) are further evidence that the enhanced ferrimagnetic fraction spans the SSD/SP boundary.

## TEMPERATURE-DEPENDENT MAGNETIC BEHAVIOUR

### Low-temperature magnetic susceptibility

After cooling to liquid nitrogen temperature (77 K), the magnetic susceptibility of samples was monitored on warm-up to room temperature using a water-jacketed susceptibility probe.

The reported behaviour of different magnetic fractions is shown in Fig. 4. Paramagnetic, cation-deficient magnetite, Fe oxide grains with ilmenite lamellae, and superparamagnetic ( $< 80 \text{ \AA}$ ) haematite are all reported to show a decrease in susceptibility on warming from liquid nitrogen tempera-

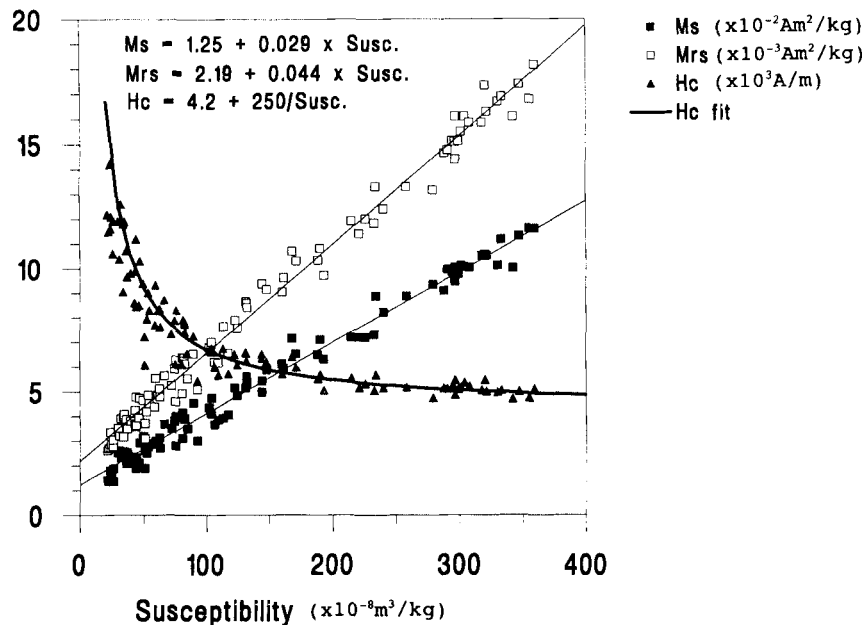


**Figure 3.** Variation of hysteresis parameters coercivity ( $H_c$ ), saturation magnetization ( $M_s$ ), and saturation remanence ( $M_{rs}$ ) with low-field susceptibility.

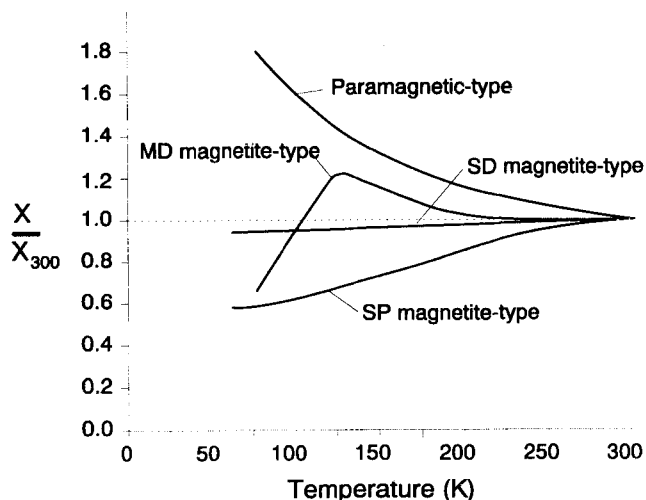


**Figure 4.** Reported low-temperature susceptibility behaviour for different magnetic fractions.

tures; SSD magnetite and maghemite have an almost constant relationship with temperature; multidomain (MD) magnetite shows a peak at 120 K; and SP/SSD magnetite shows an increase on warming (Takada & Kawai 1962; Senanayake & McElhinny 1981; Radhakrishnamurty & Subbarao 1990). The paramagnetic contribution ('Curie Law' behaviour) was subtracted using the VSM measurement of high-field susceptibility as an estimate of paramagnetic susceptibility.

A trend in behaviour emerges for samples with increasing magnetic susceptibility (Fig. 5). Samples with the lowest susceptibility values show a peak at 120 K and a general 'paramagnetic-type' decrease on warm-up. Removal of the paramagnetic contribution reveals the underlying behaviour is of 'SD/MD magnetite-type'. At the other extreme, samples with the highest susceptibilities show 'SP/SSD magnetite-type' behaviour. Samples with intermediate

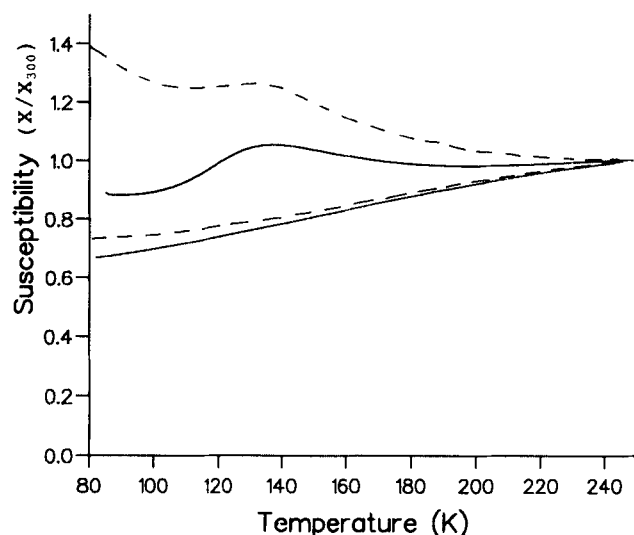


**Figure 5.** Low-temperature susceptibility behaviour for samples with low and high room-temperature magnetic susceptibility: before (dashed line) and after (solid line) the subtraction of a paramagnetic contribution.

susceptibilities show behaviour that lies between these two extremes. The loss of a MD peak in samples with strongly enhanced susceptibilities could either represent a shift in ferrimagnetic grain size (to finer grains), or the dominance of 'SP/SSD magnetite-type' behaviour.

#### Low-temperature thermal demagnetization of SIRM

Remanence was measured at low temperature using a superconducting susceptometer (at the Institute for Rock Magnetism, University of Minnesota). A saturating remanence (SIRM) was produced (2.5 Tesla applied field) in samples cooled to 5 K. The temperature was then stepped in 5 K intervals up to room temperature; the remanence (in zero field  $< 300 \mu\text{T}$ ) being measured several times at each temperature. The overall time for a complete run was approximately 3 hr.

For samples with low magnetic susceptibility, a clearly defined Vewrey transition is observed (Fig. 6), indicating that some pure unoxidized magnetite is present. On the other hand, samples with strongly enhanced susceptibilities show behaviour that is dominated by highly oxidized magnetites/maghemites (Özdemir, Dunlop & Moskowitz 1993). All samples show a strong decrease in remanence at low temperature.

#### High-temperature magnetization

The high-field (60–530 mT) magnetization behaviour of loess samples was measured over the temperature range 40–700 °C, using a horizontal translation balance. The time for one heating/cooling cycle (in air) was approximately 30 min. The paramagnetic contribution to the magnetization

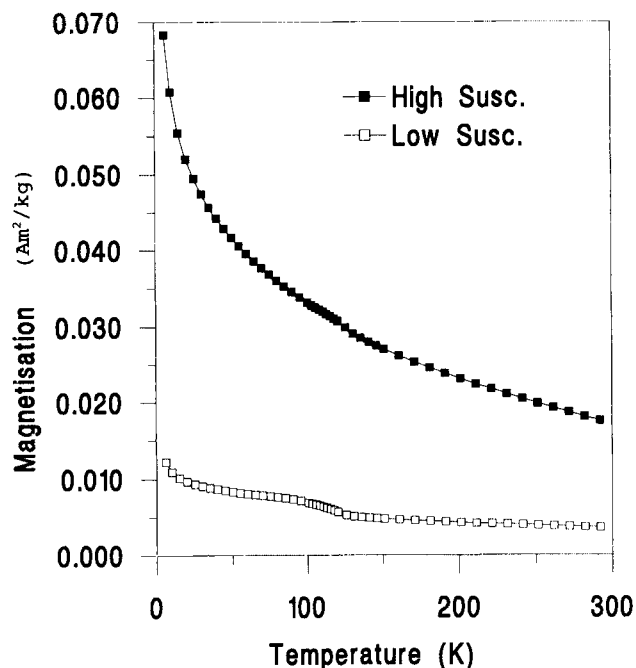


**Figure 6.** Thermal demagnetization of a saturation remanence (SIRM) given at 5 K for samples with low and high susceptibilities.

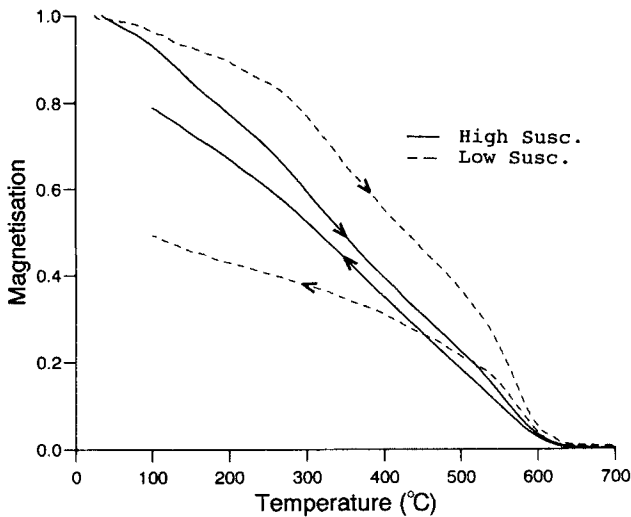


**Figure 7.** High-field (420 mT) thermomagnetic behaviour for samples (heated in air) with low (dashed line) and high (solid line) room-temperature magnetic susceptibility. The paramagnetic contribution has been subtracted in both cases.

curve was subtracted\* in each case using room-temperature VSM measurements of high-field susceptibility.

Again, samples show a trend in behaviour related to the initial magnetic susceptibility of the sample (Fig. 7). Samples with low susceptibility show irreversible behaviour, a distinct change of slope around 350 °C, and Curie temperatures ~600 °C, characteristic of cation deficient magnetite/maghemite (Stacey & Banerjee 1974; Özdemir & Banerjee 1984). At the other extreme, samples with relatively high susceptibility show a greater reversibility but with similar Curie temperatures. Reversibility would indicate pure, unoxidized magnetite as the dominant fraction. However, the shape of the curves and the high Curie temperature is anomalous. The very linear behaviour with temperature is a deviation from the spontaneous magnetization curve for pure magnetite and the Curie temperature is too high (for pure bulk magnetite  $T_c = 585$  °C). Samples showing this anomalous behaviour were reheated and subjected to different applied fields (60–530 mT). Little variation in behaviour was observed. On a subsequent series of six heating cycles there was no further loss in magnetization and the shape of the curves remained unchanged.

## DISCUSSION

The trend in magnetic behaviour with susceptibility highlights that susceptibility variation is associated with a change in ferrimagnetic concentration. Moreover, given that our samples represent extremes in loess type, this association appears to be universal throughout the loess plateau. However, an explanation involving only a single magnetic component is insufficient to explain the magnetic behaviour in detail. Two ferrimagnetic components appear

\* Room temperature paramagnetic magnetization  $M_p = X_{\text{hfd}} \times H$  where  $X_{\text{hfd}}$  is the VSM measurement of high-field susceptibility,  $H$  is the applied field. An inverse temperature relationship was used to approximate  $M_p$  over the whole temperature range.

to be present in the Chinese loess. Enhancement of the ultrafine ferrimagnetic component takes place relative to a 'background' magnetic component which shows magnetic behaviour characteristic of a coarse-grained, cation-deficient magnetite.

Low-temperature thermal demagnetization of SIRM strongly indicates that any magnetite present in samples that have enhanced susceptibilities is highly oxidized. The strong decrease in remanence, for all samples, at low temperature is rather puzzling. Özdemir *et al.* (1993) reported the similar phenomena for their oxidized fine-grained magnetites, and gave an explanation involving the unblocking of interacting SP/SSD grains. These grains, they suggested, had formed by the stretching and cracking of a surface layer due to a difference in lattice constant between the oxidized surface and the less oxidized core. For our samples with the highest susceptibilities, the gradient of the demagnetization curve is roughly proportional to  $-1/T$  and there is very little divergence from this behaviour or a flattening at low temperature which would indicate the progressive unblocking of a grain-size distribution.

High-temperature magnetization reveals that samples with strongly enhanced susceptibilities show reversible, linear behaviour and high Curie temperatures. If we consider (from the other magnetic measurements) that this magnetic behaviour is dominated by ultrafine ferrimagnets, then the high thermal stability is quite unexpected. Ultrafine magnetite is quickly oxidized to maghemite when exposed to air (Özdemir *et al.* 1993) and maghemite is reportedly metastable, inverting to haematite on heating >550 °C (Stacey & Banerjee 1974). However, the inversion temperature of maghemite is something of a controversial issue. For example, Taylor & Schwertmann (1974b) reported an inversion temperature between 748 and 780 °C for naturally occurring soil maghemites, based on DTA analysis. In a detailed study of synthetic pure and trace element-substituted maghemites, Sidhu (1988) showed that alteration occurred rapidly (~40 per cent in 20 min) above ~500 °C. Substitution by aluminium can enhance the thermal stability of maghemite (De Boer & Selwood 1954) and may be one possible explanation for the reversibility observed for our samples. Aluminium is also reported to lower the Curie temperature (Thompson & Oldfield 1986), which is consistent with our observations for maghemite  $T_c \approx 590$  °C, Aharoni & Schieber 1962; 645 °C, Özdemir & Banerjee 1984; 747 °C, Brown & Johnson 1962).

Spin-canting in the surface layer of maghemite has been reported in a number of papers (see Haneda's 1987 review on the magnetism of fine particles). With decreasing particle size the influence of surface becomes more significant. In the case of spin-canting, the net magnetization of a grain is reduced, depending on the layer thickness, the canting angle and the grain volume. How this situation develops with temperature is still not clear, but it may lead to a deviation from the magnetic behaviour seen for bulk maghemite.

However, there may be an alternative explanation. Ultrafine  $\text{Fe}_2\text{O}_3$  in the size range 50–500 Å is reported to exhibit some interesting properties. In particular, between 100 and 300 Å, maghemite ( $\gamma\text{Fe}_2\text{O}_3$ ) appears to be the energetically favoured phase (Krupyanskii & Suzdalev 1974; Ayyub *et al.* 1988). Above 300 Å haematite ( $\alpha\text{Fe}_2\text{O}_3$ ) is the stable phase, and below 100 Å an amorphous (Ayyub *et al.*

1988) or distorted (Krupyanskii & Suzdalev 1974) paramagnetic 'x-phase' persists. Ayyub *et al.* (1988) concluded that the preference for the  $\gamma$ -phase is due to an increase in the lattice constant for decreasing grain sizes. Furthermore, they found a positive correlation between the Mössbauer hyperfine field and grain size, suggesting that changes in unit-cell size have an effect on the superexchange interaction. A decrease in the spin coupling could be reasonably expected to lower the Curie temperature. Thus, our anomalous thermomagnetic curves could be explained in several ways.

(1) With increasing temperature, there is a thermal expansion of the unit-cell volume, resulting in some grains undergoing a  $\gamma$ - $x$  reversible phase change with a consequent loss in magnetization.

(2) With a range of  $\gamma\text{Fe}_2\text{O}_3$  grain sizes, there will be range of unit-cell sizes and an associated distribution of Curie temperatures. Hence, the shape of the cumulative curve would deviate from the behaviour for bulk maghemite (with only a single Curie temperature).

(3) Unit-cell size may be strongly temperature dependent, within the  $\gamma$ -phase grain-size range, resulting in a stronger decrease in magnetization with temperature.

An obvious requirement for all three explanations is that thermomagnetic behaviour is reversible. More specifically, maghemite of this particular grain-size range must not invert to haematite during heating to 700 °C. According to Ayyub *et al.* (1988), the  $x$  and  $\gamma$  phases are metastable and will invert to  $\alpha\text{Fe}_2\text{O}_3$  above  $\sim 420$  °C, but present little evidence that this is the case for the particular grain-size range in question. According to Krupyanskii & Suzdalev (1974), 'the term "metastable phase" must be applied only to (those) phases in bulk material, since in our experiments all transitions  $x$ - $\gamma$  and  $\gamma$ - $\alpha$  are reversible (for definite particle dimension).' They point out that small maghemite grains may, through sintering, increase in size during heating and consequently invert to haematite. We can infer from this that if the heating times are short, reversibility may be possible.

If we accept that maghemite is the stable phase for grain sizes in the range  $\sim 100$ – $300$  Å, then it is, perhaps, no surprise that we appear to have an enhanced ferrimagnetic fraction of a particular grain-size range which spans the SSD/SP boundary (for maghemite the critical diameter for superparamagnetism is probably similar to that of magnetite  $d_{\text{crit}} \approx 250$ – $300$  Å, Dunlop 1981). The concentration of a maghemite component would be simply governed by the concentration of  $\text{Fe}_2\text{O}_3$  in this size range.

## CONCLUSION

There has been much speculation over the origin of the ultrafine ferrimagnetic fraction in the Chinese loess. Our measurements have highlighted that ferrimagnetic concentration, rather than a change in grain size, is the controlling factor in magnetic susceptibility enhancement throughout the loess plateau. In trying to explain anomalous thermomagnetic behaviour, the possibility of a stable ultrafine  $\gamma\text{Fe}_2\text{O}_3$  phase was considered. The particular grain-size range, over which  $\gamma$  is the stable phase of  $\text{Fe}_2\text{O}_3$

(at room temperature), is consistent with grain-size estimations made from room-temperature magnetic measurements. The effect of climate on magnetic susceptibility is likely to be through the influence of rainfall and temperature on pedogenesis. Any process that results in the production of ultrafine  $\text{Fe}_2\text{O}_3$ —including the breakdown of iron-containing silicates/clays, oxidation of magnetites and dehydration of oxyhydroxides—is a possible mechanism for susceptibility enhancement.

## ACKNOWLEDGMENTS

We would like to thank Professor E. Derbyshire, Professor An Zisheng and Professor Wang Jingtai for helping us to collect samples in China, the NERC for supporting JKE with a studentship, and Xu Tungsheng for help with the sampling. Thanks also to the Institute for Rock Magnetism (IRM) in Minneapolis for the use of its facilities and for providing J.K.E. with some of the expenses for a 10 day visit as a 'Visiting Fellow'. The IRM is funded by the Keck foundation, the National Science Foundation, and the University of Minnesota. This work is supported by a NERC palaeoclimate grant (GST/02/540) and a British Council link scheme.

## REFERENCES

- Aharoni, E.H.F. & Schieber, M., 1962. Some properties of  $\gamma\text{Fe}_2\text{O}_3$  obtained by hydrogen reduction of  $\alpha\text{Fe}_2\text{O}_3$ , *J. Phys. Chem. Solids*, **23**, 545–554.
- Anand, R.R. & Gilkes, R.J., 1987. The association of maghemite and corundum in Darling Range laterites, Western Australia, *Aust. J. Soil Res.*, **35**, 301–311.
- Ayyub, P., Multani, M., Barma, M., Palkar, V. R. & Vijayaraghavan, R., 1988. Size-induced structural phase transitions and hyperfine properties of microcrystalline  $\text{Fe}_2\text{O}_3$ , *J. Phys. C: Solid State Physics*, **21**, 2229–2245.
- Brown, W.F., Jr & Johnson, C.E., Jr, 1962. Temperature variation of saturation magnetisation of gamma-ferric oxide, *J. appl. Phys.*, **33**(9), 2752–2754.
- Burbank, D.W. & Li, J., 1985. Age and palaeoclimatic significance of the loess of Lanzhou, north China, *Nature*, **316**, 429–431.
- De Boer, F. & Selwood, P.W., 1954. The activation energy for the solid state reaction  $\gamma\text{Fe}_2\text{O}_3 \rightarrow \alpha\text{Fe}_2\text{O}_3$ , *J. Am. chem. Soc.*, **76**, 3365.
- Dunlop, D.J., 1981. The rock magnetism of fine particles, *Phys. Earth planet. Inter.*, **26**, 1–26.
- Fassbinder, J.W.E., Stanjek, H. & Vali, E., 1990. Occurrence of magnetic bacteria in soil, *Nature*, **343**, 161–163.
- Guo, Z., Nicolas, F. & An, Z., 1991. Genetic types of the Holocene soil and the Pleistocene palaeosols in the Xifeng loess section in central China, in *Loess, Environment and Global Change*, pp. 93–111, ed. Liu, T., XIII Inqua Congress Science Press, China.
- Haneda, K., 1987. Recent advances in the magnetism of fine particles, *Can. J. Phys.*, **65**, 1233–1244.
- Heller, F. & Liu, T., 1984. Magnetism of Chinese loess deposits, *Geophys. J.R. astr. Soc.*, **77**, 125–141.
- Heller, F. & Liu, T., 1986. Palaeoclimatic and sedimentary history from magnetic susceptibility of loess in China, *Geophys. Res. Lett.*, **13**, 1169–1172.
- Krupyanskii, Y.F. & Suzdalev, I.P., 1974. Magnetic properties of ultrafine iron oxide particles, *Sov. Phys. JETP*, **38**, 859–864.
- Kukla, G., Heller, F., Liu, X.M., Xu, T.S. & An, Z.S., 1988. Pleistocene climates in China dated by magnetic susceptibility, *Geology*, **16**, 811–814.

- Liu, T., 1985. *Loess and the Environment*, China Ocean Press Beijing.
- Liu, T.S., An, Z.S., Yuan, B.Y. & Han, J.M., 1985. The loess-palaeosol sequence in China and climatic history, *Episodes*, **8**, 21–28.
- Maher, B.A. & Taylor, R.M., 1988. Formation of ultrafine-grained magnetite in soils, *Nature*, **336**, 368–370.
- Maher, B.A. & Thompson, R., 1991. Mineral magnetic record of the Chinese loess and palcosols, *Geology*, **19**, 3–6.
- Özdemir, Ö. & Banerjee, S.K., 1984. High temperature stability of maghaemite, *Geophys. Res. Lett.*, **11**(3), 161–164.
- Özdemir, Ö., Dunlop, D.J. & Moskowitz, B.M., 1993. The effect of oxidation on the Vewrey transition in magnetite, *Geophys. Res. Lett.*, **20**(16), 1671–1674.
- Radhakrishnamurthy, C. & Subbarao, K.V., 1990. Palaeomagnetism and rock magnetism of the Deccan traps, *Proc. Indian Acad. Sci., (Earth planet Sci.)*, **99**(4), 669–680.
- Rolph, T.C., Shaw, J., Derbyshire, E. & Wang, J., 1989. A detailed geomagnetic record from Chinese loess, *Phys. Earth planet. Inter.*, **56**, 151–164.
- Rolph, T.C., Shaw, J., Derbyshire, E. & Wang, J., 1993. The magnetic mineralogy of a loess section near Lanzhou, China, in *The Dynamics and Environment Context of Aeolian Sedimentary Systems*, ed. Pye, K., Geological Society Special Publication No. 72, 311–323.
- Senanayake, W.E. & McElhinny, M.W., 1981. Hysteresis and susceptibility characteristics of magnetite and titanomagnetites: interpretation of results from basaltic rocks, *Phys. Earth planet. Inter.*, **26**, 47–55.
- Sidhu, P.S., 1988. Transformation of trace element-substituted maghemite to hematite, *Clays and Clay Miner.*, **36**(1), 31–38.
- Stacey, F.D. & Banerjee, S.K., 1974. *The Physical Principles of Rock Magnetism, Developments in Solid Earth Geophysics* Vol. 5, Elsevier Scientific Publishers, Amsterdam.
- Takada, T. & Kawai, N., 1962. Magnetism in ultra fine oxide particles, *J. Phys. Soc. Japan*, **17**–**B1**, 691–694.
- Taylor, R.M. & Schwertmann, U., 1974a. Maghemite in soils and its origin, I. Properties and observations on soil maghemites, *Clay Miner.*, **10**, 289–298.
- Taylor, R.M. & Schwertmann, U., 1974b. Maghemite in soils and its origin, II. Maghemite syntheses at ambient temperature and pH7, *Clay Miner.*, **10**, 299–310.
- Taylor, R.M., Maher, B.A. & Self, P.G., 1987. Magnetite in soils: I. The synthesis of single-domain and superparamagnetic magnetite, *Clay Miner.*, **22**, 411–422.
- Thompson, R. & Oldfield, F., 1986. *Environmental Magnetism*, Allen & Unwin, London.
- Zheng, H., An, Z. & Shaw, J., 1992. New contributions to Chinese Plio-Pleistocene magnetostratigraphy, *Phys. Earth planet. Inter.*, **70**, 146–153.